Highly Consistent Atmospheric Pressure Synthesis of Carbon Nanotube Forests by Mitigation of Moisture Transients

Citation: Li, Jinjing, Mostafa Bedewy, Alvin Orbaek White, Erik S. Polsen, Sameh Tawfick, and A. John Hart. "Highly Consistent Atmospheric Pressure Synthesis of Carbon Nanotube Forests by Mitigation of Moisture Transients." The Journal of Physical Chemistry C 120, no. 20 (May 17, 2016): 11277–11287.

As Published: http://dx.doi.org/10.1021/ACS.JPCC.6B02878

Publisher: American Chemical Society (ACS)

Persistent URL: http://hdl.handle.net/1721.1/119379

Version: Author's final manuscript: final author's manuscript post peer review, without publisher's formatting or copy editing

THE JOURNAL OF PHYSICAL CHEMISTRY C

Article

pubs.acs.org/JPCC

Highly Consistent Atmospheric Pressure Synthesis of Carbon Nanotube Forests by Mitigation of Moisture Transients

Jinjing Li,[†] Mostafa Bedewy,[†,‡,§] Alvin Orbaek White,[‡] Erik S. Polsen,[†] Sameh Tawfick,[†,‡,∥] and A. John Hart*[,†,‡]

[†]Department of Mechanical Engineering, University of Michigan, Ann Arbor, Michigan 48109, United States

[‡]Department of Mechanical Engineering and Laboratory for Manufacturing and Productivity, Massachusetts Institute of Technology, Cambridge, Massachusetts 02139, United States

Supporting Information

ABSTRACT: Consistent synthesis of carbon nanotubes (CNTs) using laboratory-scale methods is essential to the development of commercial applications, particularly with respect to the verification of recipes that achieve control of CNT diameter, chirality, alignment, and density. Here, we report that transients in the moisture level and carbon concentration during the chemical vapor deposition (CVD) process for vertically aligned CNT "forests" can contribute significantly to run-to-run variation of height and density. Then, we show that highly consistent CNT forest growth can be achieved by physically decoupling the catalyst annealing and hydrocarbon exposure steps, to allow the gas composition to stabilize between the steps. This decoupling is achieved using a magnetically actuated transfer arm to move the substrate rapidly into and out of the CVD reactor. Compared to a reference process where the sample resides in the furnace throughout the process, the decoupled method gives 21% greater CNT forest height, reduces the run-to-run variance of height by 76%, and results in forests with improved vertical alignment (Herman's orientation parameter of 0.68 compared to 0.50). Building on this foundation, we study the influence of the moisture level during the CNT growth step and find a 30% improvement in growth rate going from the baseline condition (<15 ppm) to 40 ppm. Interestingly, however, the increased moisture concentration does not improve the catalyst lifetime or the CNT forest density, warranting further study of the role of moisture on CNT nucleation versus growth.

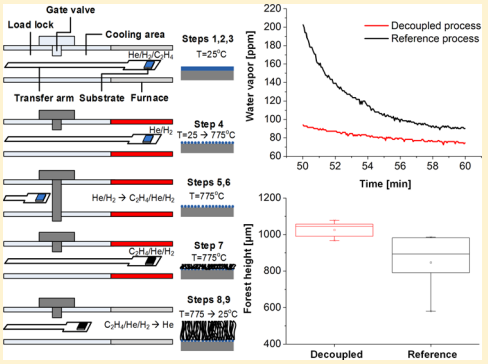

1. INTRODUCTION

Nearly two decades of research on the synthesis and applications of vertically aligned carbon nanotubes (CNTs) has led to much empirical understanding of the coupled chemical and mechanical process of CNT nucleation and self-organization.[1−5] This resulted in a myriad of recipes for substrate preparation and chemical vapor deposition to achieve control of the key attributes such as CNT diameter and areal density.[6−9] However, a common frustration among researchers, and critical issue for effective translation of research, is the lack of consistency of key production metrics (e.g., height, density) when using laboratory-scale synthesis equipment.

As in many chemical vapor deposition (CVD) processes, it is critical to control the level of oxygen-containing impurities and/or additives in the CNT synthesis reactor atmosphere. In particular, CNT synthesis involves complex hydrocarbon reactions in the gas-phase, and the typical use of supported metallic nanoparticles to seed and mediate CNT growth means that the reaction pathways of CNT formation have proven largely impossible to interpret with certainty. Further, the multiple pathways of carbon during the CNT synthesis process, beginning with nucleation of graphitic layer(s) on the catalyst and continuing with lift-off and steady growth of the CNT, complicate our understanding of the overall process and specifically the mechanisms limiting CNT growth rate and lifetime. These points aside, robust process control affords both clearer scientific interpretation as well as improved engineering for applications.

In particular, since Hata and colleagues reported that rapid atmospheric pressure synthesis of millimeter-tall CNT forests can be aided by ∼100 ppm levels of moisture in the CVD system,[10] it has been suggested that CNT growth is influenced by moisture levels in the thousands of ppm,[11] hundreds of ppm,[12] less than ppm levels,[13] and even less than ppb levels.[14] Proposed mechanisms by which moisture and oxygen influence CNT synthesis include modulation of the growth rate, etching of amorphous carbon that may form on the catalyst, and mitigation of Ostwald ripening which leads to deactivation of smaller catalyst particles. For example, Zhang et al. suggested the presence of oxygen provides a carbon-rich and hydrogen-deficient condition to favor the formation of an sp^2-like graphitic structure.[15] On the other hand, Amama et al. observed moisture during the CVD process can inhibit Ostwald ripening due to the ability of oxygen and hydroxyl species to reduce the

Received: March 20, 2016
Revised: May 4, 2016

DOI: 10.1021/acs.jpcc.6b02878
J. Phys. Chem. C XXXX, XXX, XXX−XXX

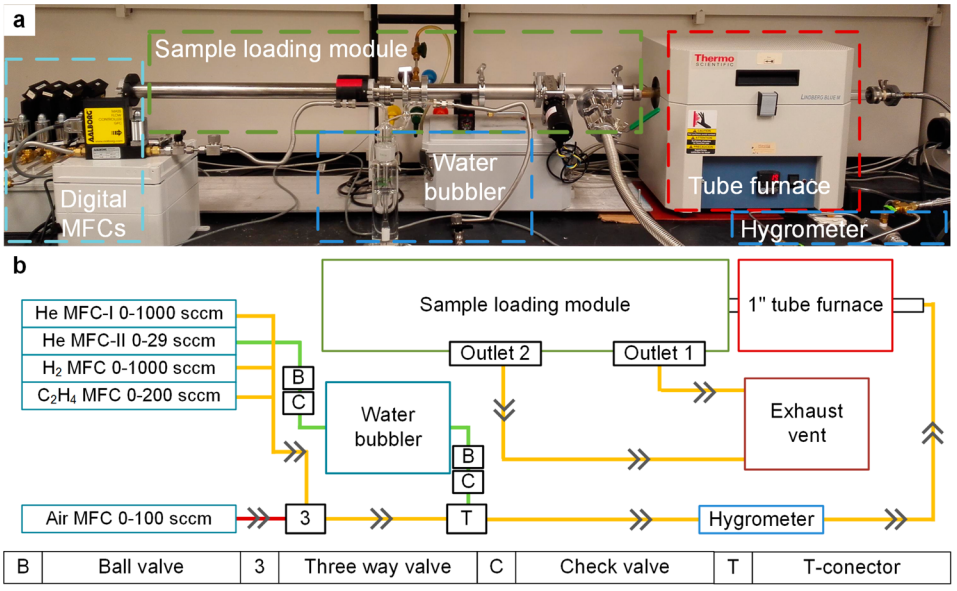

Figure 1. System for decoupled moisture-controlled chemical vapor deposition. (a) Photo of the entire system labeled with submodules. (b) Schematic of the system labeled with flow directions through stainless steel piping.

diffusion rate of catalyst atoms.[16] Moreover, it has been found that the consistency of atmospheric pressure CVD of CNT forests, as measured by the CNT forest height and density, is influenced by run-to-run moisture fluctuations in the reactor.[17] These fluctuations can be caused by diffusion of ambient moisture through polymer tubing, ~10−100 ppm levels of moisture present in high purity gas supplies, and adsorption of moisture inside the reactor during sample exchange.

In a typical CNT synthesis procedure, substrates are first annealed in a hydrogen-containing atmosphere, followed by addition of the carbon source for the CNT growth stage. The intrinsic response rate of electronic mass flow controllers (MFCs) can be as slow as several seconds; the transient chemical composition of the mixed gases when the composition is changed (e.g., from the annealing to growth stage) can persist over several tens of seconds due to the flow rate (e.g., ~500 sccm) relative to the volume of the quartz tube (~200−300 cm^3 for 25 mm diameter). This results in an even longer transient in the chemistry of the atmosphere, and in particular the composition of thermally generated hydrocarbons that are known to influence CNT growth. Previous research by Meshot et al. observed that CNT forest growth rate is related to the partial pressure of C_2H_4.[18] Therefore, it can be imagined that the rate of change between exposure conditions for the annealing and growth steps would influence the outcome of the CVD process, such as by governing the rate at which CNTs consecutively nucleate from the catalyst particle population on the substrate.

In order to understand these influences in more detail and develop principles for scalable manufacturing of CNT forests, it is essential to have a consistent baseline process upon which the influence of multivariate conditions can be evaluated, and through which samples for subsequent processing can be reliably made. In this study we explore the influence of moisture transients on the CVD process and develop protocols for highly consistent CNT growth based on stabilization of moisture and rapid sample insertion. First, we find that decoupling the annealing and growth stages by rapid sample insertion increases the mean forest height by 21.0% and reduces run-to-run variation in height by 75.7%. Small angle X-ray scattering (SAXS) was used to measure CNT alignment,[19] and results showed that forests produced by the decoupled recipe have improved CNT alignment (Herman's orientation parameter 0.62−0.68) compared to forests obtained from a reference CVD process (0.44−0.50). Then, the influence of moisture concentration on the steady state growth stage is studied when the moisture level during annealing is held constant. A 30% improvement in growth rate is observed going from the baseline condition (<15 ppm) to 40 ppm, compared to less than 10% of additional improvement when further increasing the moisture concentration to 450 ppm. Interestingly, the increased moisture concentration does not improve the catalyst lifetime, nor CNT forest density.

2. METHODS

2.1. Substrate Preparation. Supported catalyst thin films were deposited by sputtering (Lab18, Kurt Lesker) Al_2O_3 (10 nm) followed by Fe (1 nm) on thermally oxidized (100) silicon wafers.[5] The silicon wafers coated with the catalyst were then cut into rectangular pieces (4 × 8 mm) using an automatic dicing saw (ADT-Dicing, model 7100). The wafer pieces were sonicated in a beaker containing acetone, for 8 min (Crest Ultrasonics model 1100D, power setting 6), after which the acetone was discarded and replaced with fresh acetone, and then sonication was repeated for 8 additional minutes at the same setting. The sonication procedure was repeated once again using methanol, and then 2-propanol, and then the substrate was removed using tweezers and dried in a gentle nitrogen stream.

2.2. CNT Synthesis. CNT synthesis was performed in a hot-walled CVD system, which was built in-house. The system consists of a horizontal tube furnace (Thermo Scientific Lindberg/Blue M Mini-Mite, FT55035 COMA-1), fitted with a quartz tube (25 mm OD, 22 mm ID), and a custom-built sample loading system attached to the furnace (Figure 1). The CVD system is modular, including a CNT synthesis module, a sample loading module, and a moisture control module.

DOI: 10.1021/acs.jpcc.6b02878
J. Phys. Chem. C XXXX, XXX, XXX−XXX

A schematic of the CVD system is shown in Figure 1b. The CNT synthesis module includes the mass flow controllers and tube furnace (Lindberg MiniMite). Five digital MFCs (Aalborg) are used to control the gas flows: helium (He; main stream, dry), helium (through water bubbler), hydrogen (H_2), ethylene (C_2H_4), and air. A three-way valve is installed between the air MFC and other MFCs, so the oxidizer (air) is never delivered together with flammable gases (H_2 and C_2H_4). The gas flow rates as well as the furnace temperature were controlled and recorded using a LabVIEW program that was developed in-house.

A major component in the sample loading module is a vacuum compatible transfer arm (VF-1695-18, Huntington Mechanical Laboratories), which has a stainless steel shaft that is magnetically coupled to a manually movable ring located outside of the sealed chamber. The end of the transfer arm is fitted with a custom quartz boat (18 × 75 mm, Figure S1, Figure S2), which holds the catalyst-coated sample. The temperature of this sample holder attached to the transfer arm was measured by affixing a thermocouple (Omega, XCIB-J-2-6-3) connected to a data acquisition card (National Instruments, USB-TC01). To monitor the moisture level entering the furnace, a hygrometer (Kahn Cermet II) was installed immediately upstream of the inlet to the furnace tube, and the hygrometer readings were also recorded by LabVIEW. More detailed information about the moisture control module can be found in the Supporting Information (Figure S3).

CNT synthesis according to the "decoupled recipe" is performed as follows (Figure 2):

– Step 1 (sample loading): The catalyst-coated substrate is placed onto the quartz boat attached to the transfer arm, the system is sealed, and the arm is manually positioned such that the leading edge of the sample is at the desired location (7 cm downstream from the furnace control thermocouple, unless otherwise noted).

– Step 2 (purging): The system is purged with He (100 sccm, 99.999% Cryogenic Gases), H_2 (400 sccm, 99.998%, Cryogenic Gases), and C_2H_4 (150 sccm, 99.5%, Cryogenic Gases) for 5 min at room temperature. Next, the flow is switched solely to He (1000 sccm) for 5 min. Purging all gases improves consistency by eliminating the effect of moisture which diffuses into the system when the furnace is not in use and/or open to the environment.

– Step 3 (filling): Prior to heating of the furnace, the flow is switched to H_2 (400 sccm) and He (100 sccm) and held for 10 min at room temperature.

– Step 4 (catalyst annealing): The furnace is then heated to 775 °C over 10 min. Upon reaching the set point temperature the flow is held for a further 10 min. During this stage, the catalyst film is chemically reduced and Fe nanoparticles are formed by dewetting.

– Step 5 (removal): The transfer arm is then used to move the sample from the heated area of the furnace into the load lock area, at which point the gate valve is closed immediately, allowing the sample to cool in the same atmosphere in which it was annealed. Closure of the gate valve at this time did not measurably influence the final CNT height or average density.

– Step 6 (atmosphere swap): Two minutes later, the flow into the furnace is changed to H_2 (100 sccm) and He (400 sccm). One minute after that, C_2H_4 (100 sccm) is added. This flow is maintained for 7 min before proceeding to the next step.

– Step 7 (CNT growth): The gate valve is opened and the transfer arm is used to insert the sample (to 7 cm downstream from the control thermocouple). This configuration is maintained for the desired growth duration (ranging from 10 s to 30 min).

– Step 8 (cooling): Upon completion of the growth duration, the furnace cover is lifted quickly, and the transfer arm is used to move the sample into the load lock position, outside the heated region of furnace. This ensures that the sample cools rapidly, while the same gas flow is maintained for an additional 5 min.

– Step 9 (unloading): The flow is switched to He only (1000 sccm); after the system has cooled to below 100 °C the load-lock is opened and the sample is removed.

After repeated synthesis experiments a dark residue of carbonaceous material is found on the walls of the quartz tube (Figure S2). To prevent contamination and achieve more consistent growth, this carbon material is removed between each experiment, by oxidation at 875 °C for 30 min in air (100 sccm, extra dry air, Cryogenic Gases).

Control experiments were also performed using a reference recipe, wherein the samples are not removed from the hot zone of the furnace between the annealing and growth stages. The reference recipe matches step 1–3 and the first 19 min of step 4 of the decoupled recipe. However, for the last minute of step 4, gas flow is changed to He (400 sccm) and H_2 (100 sccm), then 1 min later C_2H_4 (100 sccm) is added for 10 min. Upon completion of CNT growth, the furnace cover is quickly lifted, while the sample remains at the growth spot. The same gas flow is maintained for another 5 min and then changed to He (1000 sccm) for a further 5 min until the sample is removed. The gas flows, temperatures, and sample positions are listed in Table S1 and Table S2.

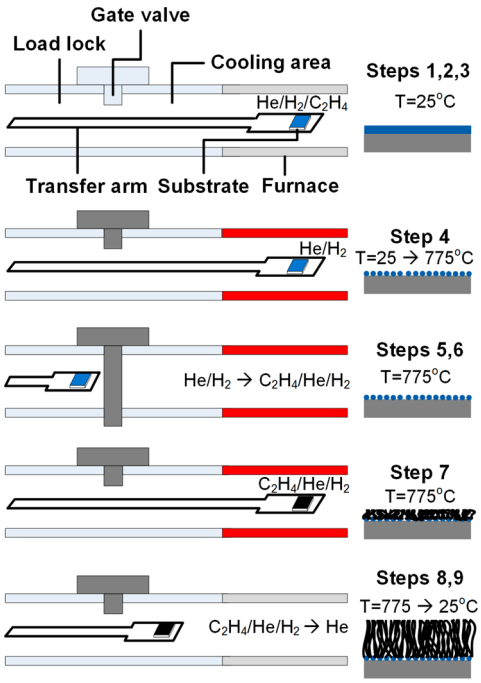

Figure 2. Schematic sequence of process steps for CNT forest synthesis according to the decoupled recipe. The transfer arm moves inward from left to right and is isolated from the furnace by a gate valve. Red and gray colors on furnace suggest the heat of furnace is turned on and off, respectively.

2.3. Moisture Control. In the results, we refer to four experimental cases: (I) humid, (II) dry, (III) dry + H_2O from

DOI: 10.1021/acs.jpcc.6b02878
J. Phys. Chem. C XXXX, XXX, XXX–XXX

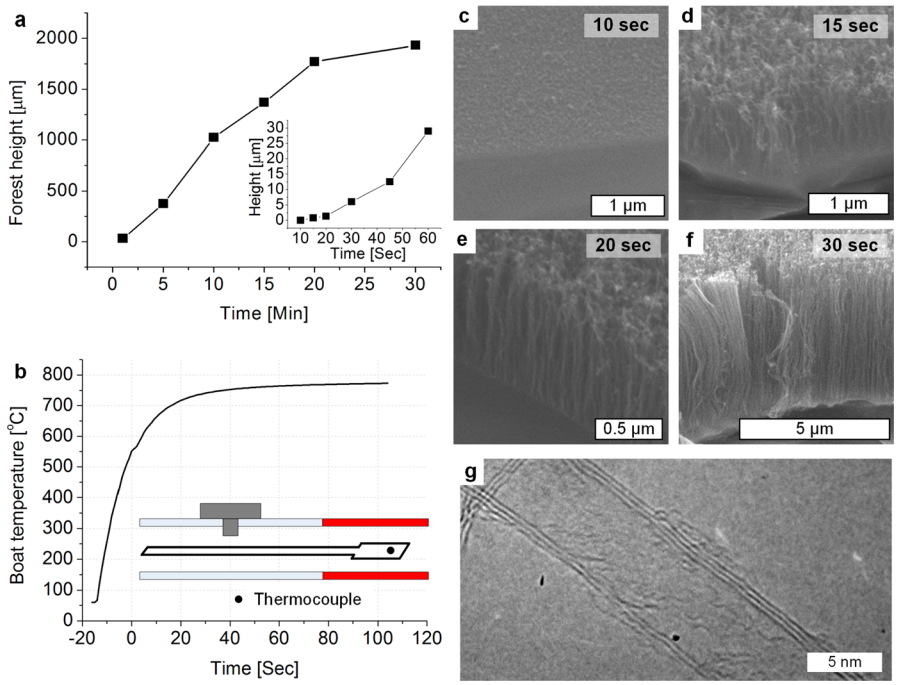

Figure 3. Height kinetics of CNT forest growth performed using the decoupled recipe. (a) Forest height versus time showing quasi-linear kinetics and abrupt termination at 20−30 min; inset showing nonlinear kinetics within the first minute of hydrocarbon exposure. (b) Temperature rise as the sample is inserted to the heated furnace, measured by attaching a thermocouple to the quartz boat (see more data in Figure S4). (c−f) SEM images of samples exposed to the hydrocarbon atmosphere for the durations noted. (g) TEM image of an individual CNT isolated from a CNT forest sample grown by the decoupled recipe for 10 min.

tank, and (IV) dry + H_2O from bubbler. The exact moisture levels measured during each stage of the process are given in the Results section.

Under case I (humid), the moisture measured in the gas mixture entering the CVD system during the annealing step (step 4) was about 250 ppm, and this resulted from a H_2 tank that contained a high moisture level of approximately 300 ppm. For the decoupled recipe, the data presented represents 10 repeated experiments, and for the reference recipe it represents 6 repeats. These experiments were performed on 8 different days during 3 months, and there was no systematic variation.

Under case II (dry), the H_2 tank used had the normally specified moisture level, which was deemed to be negligible using our hygrometer. With this, and following an overnight purge of the CVD system with flowing He (100 sccm),[17] the moisture levels measured during the annealing and growth steps were always <10 ppm for both decoupled recipe and reference method. For case II, six repeats were conducted each for decoupled recipe and reference recipe.

Under case III (dry + H_2O from tank), the overnight purge with ultrahigh purity (UHP) He was still applied. However, during the CVD cycle, a mixture of 100 ppm of H_2O in He (A31 certified mixture, CryogenicGases) was delivered to add moisture to the system. For case III, 6 repeats were conducted each for decoupled recipe and reference recipe.

Under case IV (dry + H_2O from bubbler), the moisture level was varied during the process by diverting a portion of the UHP He flow to the furnace through a bubbler. The bubbler module is described in the Supporting Information and enabled adjustment of the steady-state moisture level from approximately 10−900 ppm (Figure S3). In this case, moisture was added to the CVD system after the third minute of step 6 of the decoupled recipe, by diverting part of the He flow to the bubbler. The flow is maintained for 22 min (instead of the nominal 7 min of Step 6 to stabilize the moisture level). For each combination of CNT growth time and moisture level, only one sample was measured.

We note that the true moisture transients during our experiments are likely faster than the response of the hygrometer; this is because our experiments were carried out with 500−600 sccm total gas flow, compared to the recommended flow rate of 1000−5000 sccm for the hygrometer. For example, in experiments where the moisture recorded during growth is 22−30 ppm (case III, decoupled recipe), the measurement settled to 60−70 ppm after 90 min of continuous flow though this exceeded the duration of our experiments. Also, we note that for case I (humid), the gate valve was closed during step 5 and then opened during step 7; in cases II (dry), III (dry + H_2O from tank), and IV (dry + H_2O from bubbler) the gate valve was always kept open; this was found to not influence the CNT forest characteristics.

2.4. Characterization. Scanning electron microscopy (SEM) images of the CNT forests were taken by using a Philips XL30 FEG SEM set to a working distance of 10 mm and accelerating voltage of 10 kV. The CNT height measurements were taken a single point along the center of the leading edge of the sample. Unfortunately, we did not comprehensively measure the height variance within each CNT forest sample; however, for comparable sets of experiments performed after those presented in this study, we determined the height variance is strongly dependent on the growth conditions. In best cases with the decoupled process, the height variation is <5% within each sample. Transmission electron microscopy (TEM) images were taken using a JEOL 3011 at 300 kV and 113 mA. Atomic force microscopy (AFM) imaging was performed using a Bruker Dimension Icon in tapping mode

DOI: 10.1021/acs.jpcc.6b02878
J. Phys. Chem. C XXXX, XXX, XXX−XXX

and the scan was performed over a 500 nm by 500 nm square region. Small angle X-ray scattering was performed at the Cornell High Energy Synchrotron Source (CHESS, G1 line, wavelength 0.13 nm) with a beam size of approximately 100 μm, as described in our previous publications.[20−23] Thermogravimetric analysis (TGA) was performed with an air flow of 20 mL/min, with a heating rate of 10 °C/min.

3. RESULTS

The overarching goal of this study was to understand how the consistency of CNT forest growth was influenced by the stability of the moisture level in the CVD system and to enable precise control of the forest height using the rapid sample insertion method (the "decoupled recipe"). In what follows we describe the characteristics of CNT forests obtained using the decoupled recipe and use this recipe to investigate the influence of moisture transients on process consistency and CNT forest characteristics including height, alignment, and density.

3.1. Kinetics and Morphology of CNT Forest Growth Using the Decoupled Recipe. In order to study the kinetics of CNT growth using the decoupled recipe, samples are produced using an identical annealing sequence (steps 1−6 in Figure 2), with growth times ranging from 10 s to 30 min. Using the transfer arm (see Methods), it takes about 13−17 s to gently insert/withdraw the sample to/from the growth position in the furnace. In order to limit the variation of growth cause by manual input, the operator used a timer to control the total time of the operation and practiced to maintain a smooth motion.

As shown in Figure 3, a CNT forest is first observed at 15 s (Figure 3a inset). Here, t = 0 is defined as the instant when the sample reaches the growth position (i.e., the transfer arm stops advancing). We find that the height of forest increases nonlinearly from t = 0−60 s, and then the height kinetics becomes approximately linear until 20 min. Termination (i.e., cessation of height increase) occurs between 20 and 30 min, and the average forest height is 1.93 mm after 30 min.

We attribute the initial nonlinear CNT height kinetics to the progressive CNT activation arising from the heating rate of the substrate during insertion to the furnace, which is measured by a thermocouple attached to the quartz boat (Figure 3b, Figure S4). While the transfer arm is being inserted, the sample temperature increases from 50 to 550 °C. It takes a further 100 s for the temperature to reach the 775 °C furnace set point. Upon reaching 650−700 °C, CNT nucleation occurs, and forest growth begins when a critical density of CNTs is reached.[19] This is demonstrated by SEM examination of samples grown for different times (Figure 3c−f). After 10 s of growth (Figure 3c), the sample has a tangled film of CNTs, while after 15 s of growth (Figure 3d), a short CNT forest with vertically aligned CNTs can be observed. The time-distributed activation of catalyst particles during the initial heating and hydrocarbon exposure causes the density to reach the critical value for "lift-off" of the forest, following the initial formation of an entangled layer.

TEM analysis (Figure 3g) of a typical CNT forest produced by the decoupled recipe gave an average CNT diameter of 8.1 ± 0.5 nm, compared to a particle height of 5.8 ± 1.0 nm obtained from AFM (Figure S5). The AFM image analysis identifies each particle location via a Voronoi method and determines the height distribution by modeling each particle as a truncated sphere resting on the substrate.[23] The AFM observation of well-formed catalyst particles after the annealing step also suggests that, in our atmospheric pressure conditions, complete dewetting of the catalyst film occurs prior to withdrawal of the sample from the furnace (step 6, section 2.2).

Thermogravimetric analysis (TGA) of the samples shows only 3% of the mass is lost below 600 °C, and 96% is lost between 600 and 735 °C (Figure S6). Because an oxidation temperature greater than 500 °C is associated with less defective CNT samples,[24,25] the 96% of mass loss above 600 °C indicates that CNT forests obtained via the decoupled recipe have high purity. Raman spectra (Figure S7) show the characteristic D and G peaks that are associated with MWNTs.

We also find that CNT forests produced using the decoupled recipe have greater alignment than those produced using the reference process. For this, X-ray scattering was used to perform a quantitative nondestructive analysis of the CNT alignment and diameter distribution within samples. Using SAXS images taken at a series of vertical positions from bottom to top of each forest, we calculated the Hermans orientation parameter and fitted a mathematical model to determine the mean and variance of CNT diameter within a log-normal distribution.[19]

Figure 4a compares the Hermans parameter (f) of the CNTs versus vertical position though the forest, for four samples

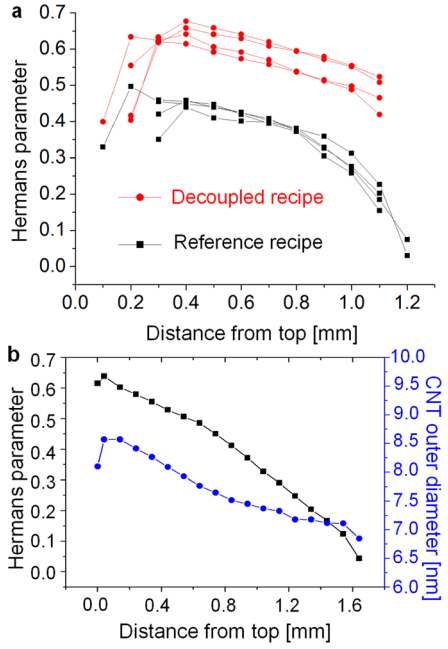

Figure 4. SAXS measurement of CNT forests. (a) Spatial mapping of alignment (Hermans orientation parameter) within CNT forests produced by the decoupled recipe, compared to reference recipe. All samples were exposed to the hydrocarbon atmosphere for 10 min. (b) Evolution of CNT diameter and alignment for a CNT forest grown by the decoupled recipe for 30 min.

chosen from the decoupled and reference groups. All samples follow the expected spatial trend of alignment within tall CNT forests grown by thermal CVD:[20,21] first, the CNT alignment increases near the top, representing an initial increase in CNT density, then the alignment gradually decreases toward the CNT−substrate interface. Comparing the decoupled and reference samples, the decoupled samples have a greater maximum value of the Hermans parameter, indicating greater alignment. Also, the rate of decay of alignment (per unit height) is lower for the decoupled samples. For the reference

DOI: 10.1021/acs.jpcc.6b02878
J. Phys. Chem. C XXXX, XXX, XXX−XXX

forests, $f < 0.1$ at the base, indicating growth self-terminated by the end of the 10 min growth step.[19] On the other hand, $f > 0.4$ at the forest base for the decoupled recipe samples grown for 10 min, indicating that growth had not terminated. This agrees with the height kinetics data.

In Figure 4b, we show the orientation trend for a CNT forest grown by the decoupled recipe for 30 min. The alignment continues to decrease toward the base of the forest, and the CNTs approach random orientation ($f = 0.0$) at the base where the collective growth has self-terminated within 30 min of hydrocarbon exposure. Corresponding SEM images may be found in Figure S8. Notably, there is also a decrease in the average CNT diameter moving downward through the height of this sample, which may be attributed to accumulating termination of CNTs arising from larger diameter catalyst particles, which was previously observed.[26] The average CNT diameter obtained from SAXS analysis of the tall forest grown by the decoupled method is 7.7 nm and assumes a log-normal diameter distribution. Detailed information on the distribution of diameter can be found in Figure S9. Also, consistent with reference work, the CNT diameter decreases (i.e., the distribution shifts to smaller values) from the top to the bottom of the forest. This can be related to the size evolution of the catalyst population as the density of growing CNTs decays with time; possible CNT deactivation mechanisms by catalyst evolution include coarsening of catalyst nanoparticles by to Ostwald ripening,[16] and the migration of catalyst atoms into the substrate.[27] By SAXS analysis, there is no apparent difference in the statistical distribution of CNT diameters between the decoupled and reference recipes.

3.2. Consistency and Influence of Moisture Transients. To assess the consistency of repeated CNT growth experiments using the decoupled recipe, we compared results to a control group obtained by a reference recipe (see Methods) where the sample remains in the CVD system during transition between the annealing and growth stages. Ten samples were produced using the decoupled recipe, and six samples were produced using the reference process, all in case I (humid), and all with a growth duration of 10 min. As shown in Figure 5, the decoupled recipe gave CNT forest height averaging 1.02 mm, which is 21% greater than forests obtained with the reference recipe (0.85 mm). Also, the standard deviation of height for the decoupled recipe was 0.04 mm (comparing average height values for each sample), which is 76% less than the standard deviation for the reference process (0.17 mm). In other words, the coefficient of variance (CV = standard deviation divided by mean height of the samples) is only 4.0% with the decoupled recipe, compared to 20% for reference forests.

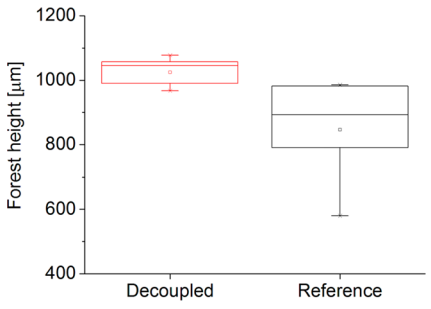

Figure 5. Run to run consistency of CNT forest height. All samples were exposed to the hydrocarbon atmosphere for 10 min.

To elucidate the reason for improved run-to-run consistency using the decoupled recipe, we measured the moisture content at each stage of the CVD process (Figure 6a, black curve) using the in-line hygrometer. The moisture level during annealing is approximately 250 ppm, yet drops when the gas mixture is switched from 400 sccm H_2 and 100 sccm He (annealing atmosphere) to 100 sccm H_2, 400 sccm He, and 100 sccm C_2H_4 (growth atmosphere, Figure 6b, c). In the reference case, the sample rests inside the furnace during this transient; when the decoupled recipe is used, the sample is withdrawn and the gas mixture stabilizes before the sample is reintroduced for CNT growth. Thus, by withdrawing the sample and allowing the moisture level to settle, we reinsert the sample at a time when the moisture level has stabilized (80−95 ppm, Figure 6c, red curve).

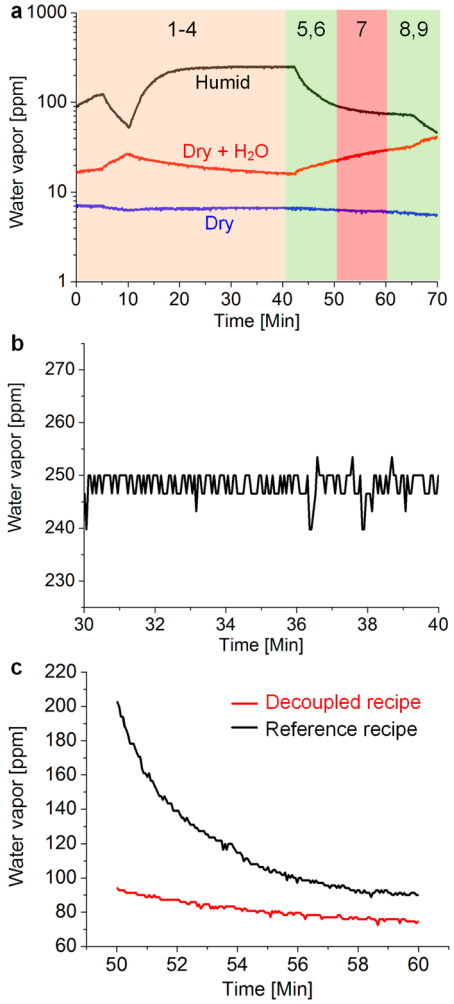

Figure 6. Moisture transients in the CVD system. (a) Moisture levels versus process time, measured at the inlet of the tube furnace, for the conditions noted and described in the text. The numbers correspond to the stages of the decoupled recipe, referring to the sample placement, as in Figure 2. (b) Close view of the stable moisture level between 30 and 40 min, at which time the annealing step (step 4, Figure 1) is performed via the decoupled recipe. (c) Comparison of moisture transients during the CNT growth step (step 7).

Therefore, our initial comparison of the decoupled versus reference methods were performed under Case I where the

DOI: 10.1021/acs.jpcc.6b02878
J. Phys. Chem. C XXXX, XXX, XXX−XXX

Table 1. Summary of Recipe Definitions and Test Cases, with Corresponding Moisture Levels Measured by Hygrometer during Annealing and Growth

case	recipe	moisture during anneal [ppm]	moisture during growth [ppm]	purpose
I: humid	decoupled	240−250	80−95	initial results with high moisture level in H_2 tank
II: dry	reference	240−250	100−210	
	decoupled	5−8	5−8	establish low and consistent moisture level
III: dry + H_2O from tank	reference	5−8	5−8	
	decoupled	15−18	22−30	add a small and constant amount of moisture
IV: dry + H_2O from bubbler	reference	15−18	15−22	
	decoupled	<15	15, 40, 120, 450	manipulate the moisture level during growth after dry annealing

anomalous moisture level from the gas tanks apparently influenced the run-to-run fluctuation of CNT forest height. It can be concluded that decoupling the annealing and growth stages by removal of the substrate from the CVD reactor during atmospheric pressure synthesis introduces two important improvements: (1) suppression of moisture transients that occur when the gas composition is switched for the growth step; (2) rapid introduction of the catalyst to a hydrocarbon-rich and chemically stable atmosphere that could enable more uniform CNT nucleation.

3.3. CNT Growth under Moisture-Controlled Conditions. The results above suggested that dedicated control of the moisture level during the CVD process (section 2.3), along with attention to the influence of transients, may enable further understanding of these principles as well as optimization of synthesis output. Accordingly, we designed a series of additional test cases (cases II, III, IV, see Methods and Table 1). For these cases, the moisture level in all gas tanks (He, H_2, and C_2H_4) were confirmed to be <10 ppm. The only exception is for case III, where a calibrated mixture of 100 sccm H_2O in He was used. A series of identical CNT growth experiments was performed with both the decoupled and reference recipes, which enabled us to further isolate the influence of overall moisture level as well as transients during the process. The results for cases I−III are summarized in Table 2, and case IV is discussed separately to follow. All experiments were performed with identical time sequences and a growth step duration of 10 min.

Table 2. Summary of Recipe Definitions and Test Cases, with Corresponding Moisture Levels Measured by Hygrometer during Annealing and Growth

	height [mm]		mass [μg]		density [μg/mm^3]	
case-recipe	average	CV	average	CV	average	CV
I-decoupled	1.02	0.04				
I-reference	0.84	0.20				
II-decoupled	0.79	0.06	402	0.07	15.9	0.10
II-reference	0.59	0.05	243	0.07	12.9	0.09
III-decoupled	1.04	0.05	633	0.06	19.0	0.04
III-reference	0.64	0.11	345	0.15	16.9	0.11

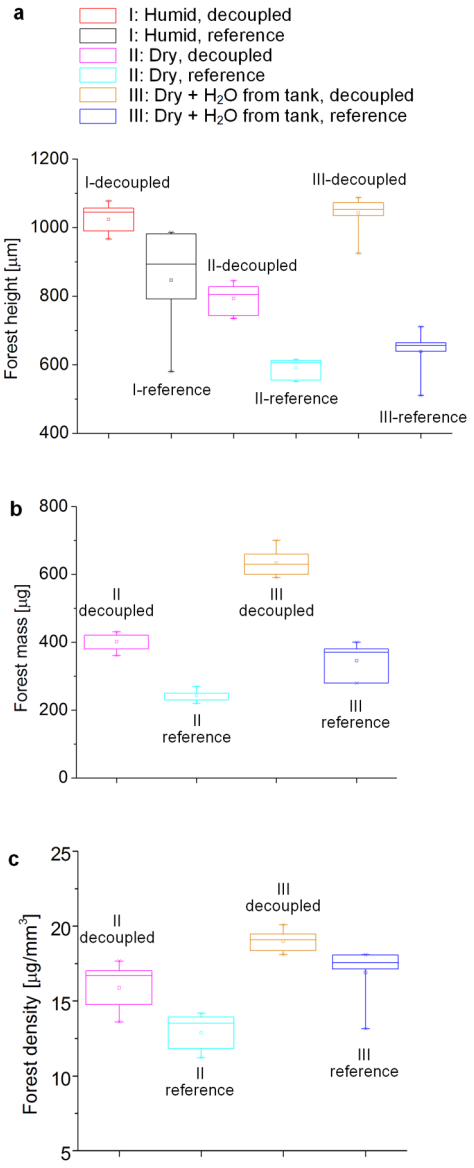

Figure 7. Box plot comparisons of CNT forest (a) height, (b) mass, and (c) density under different moisture control conditions described in the text.

Measurements of CNT forest height, mass, and average volumetric density are also summarized graphically in Figure 7. First, we find that the decoupled recipe gives taller CNT forests in all three moisture cases, as shown in Figure 7a. Moreover, when the total mass (Figure 7b) and density (Figure 7c) are compared, the decoupled recipe is superior in absolute numbers as well as lower variance. The mass and density represent approximate measures of the CNT growth yield (i.e., mass of carbon converted to CNTs by the catalyst) and the efficiency of the catalyst (i.e., number of growing CNTs in the forest).

DOI: 10.1021/acs.jpcc.6b02878
J. Phys. Chem. C XXXX, XXX, XXX−XXX

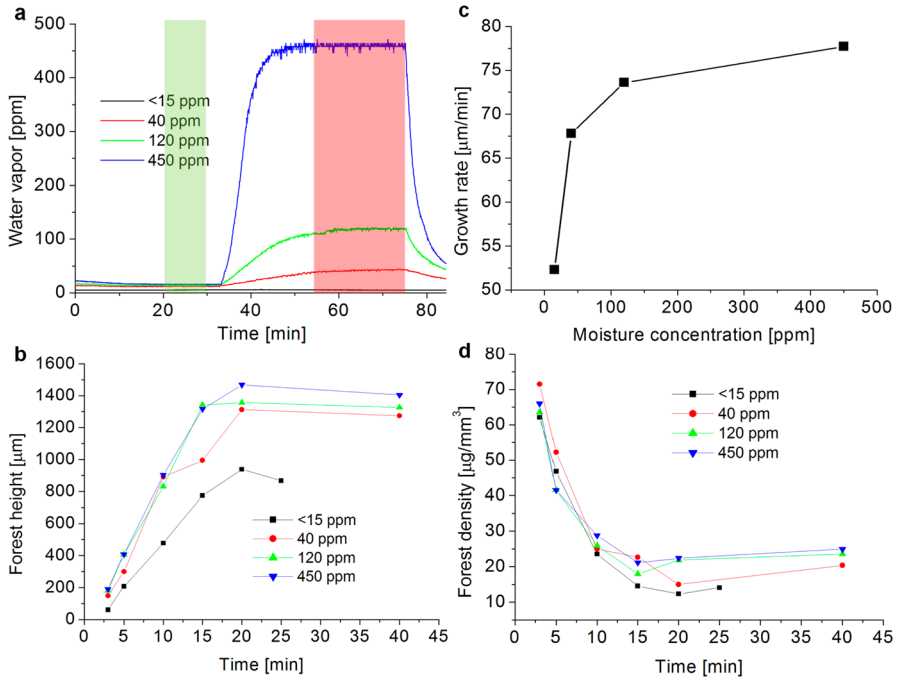

Figure 8. Influence of moisture during growth stage on CNT height kinetics via the decoupled recipe: (a) moisture transients under different flows of He to the bubbler; (b) CNT forest height versus time for each moisture level; (c) CNT growth rate (rate of height increase) versus moisture level, taken from a linear fit to the height-time data for the first 20 min of each curve in (b); (d) average density of forests versus time for the same series of experiments.

Therefore, if the synthesis goal is to maximize CNT height, mass, and density, the decoupled recipe with case III (dry + H_2O from tank) is shown to be the best among the conditions tested. The greater density of CNT forests grown by the decoupled recipe may also be attributed to the increased alignment compared to the reference recipe.

Further, by comparing the average values and variations for the decoupled and reference processes, we conclude that the greater consistency obtained with the decoupled recipe for case I is eliminated when we remove the significant moisture transient (i.e., case II). In other words, when the moisture level is well-controlled and stable throughout the process as in case II, the run-to-run variation of CNT forest height is comparable between the decoupled and the reference recipes. However, for case II the decoupled recipe still gives greater height and density, suggesting that rapid introduction of the catalyst to a stabilized gas mixture containing the hydrocarbon leads to more uniform and denser CNT nucleation. This topic requires further study. A similar comparison may be made between the decoupled and reference recipes under case III, and here the greater CNT height and density compared to all other cases may be attributed to the moisture level established using the calibrated gas source.

3.4. Influence of Steady Moisture Level on CNT Height and Density. The above results imply that, when moisture transients are eliminated, the steady-state moisture level in the CVD system influences the CNT height and mass obtained. Although, the influence of moisture level on CNT forest growth has been discussed in numerous previous studies;[10,11,28,29] however, our approach to track the moisture level throughout the process, and insert/remove the sample between steps, provides an experimental platform to systematically understand the decoupled effects of moisture on the catalyst annealing, CNT nucleation, and growth stages.

To this end, in our final case (IV), we used a bubbler to control the moisture content of the gas mixture in the CVD system (see Methods and Figure S3). By diverting a portion of the He flow through the bubbler, we found that the moisture level can be varied from <15 to 450 ppm, and the moisture level stabilizes within 15−17 min of diverting the He flow into the bubbler. With this capability along with the decoupled recipe, several CNT growth experiments were performed. The substrates were annealed with a moisture concentration <15 ppm (i.e., as in case II, with no added H_2O) in all experiments. After removal of the substrate using the transfer arm, the moisture level was changed to the desired set point by diverting He into the bubbler. Example moisture transients are shown in Figure 8a.

On the basis of the relationship between CNT height and growth time (Figure 8b), we find that the moisture level has a strong influence on the average growth rate (Figure 8c) and ultimate height, yet does not influence the apparent catalyst lifetime. Other studies of moisture-assisted CNT growth have found that moisture increases the catalyst lifetime.[10,12,13] We suspect the difference in our study is the maintenance of a constant low moisture level during the annealing step, which ensures that the size and density of catalyst particles are the same in all growth cases. The presence of moisture during annealing certainly has further effects on the diffusion and surface chemistry of the Fe/Al_2O_3 layer, and we are studying these in detail for follow-up work.

Going from the baseline condition (<15 ppm) to 40 ppm, a 30% improvement in growth rate is found. However, the relative improvements from 40 to 120 ppm and 120 to 450 ppm are only 8.6% and 5.6%, respectively. Also, based on the height and weight of each forest, we calculate the differential volumetric density (Figure 8d), which decays with time as expected. Interestingly, this deactivation behavior does not

DOI: 10.1021/acs.jpcc.6b02878
J. Phys. Chem. C XXXX, XXX, XXX−XXX

measurably depend on the moisture level in the CVD system, which indicates that while the moisture level affects the kinetics of nucleation and growth, it does not drastically alter the deactivation kinetics. However, at this point, we cannot conclude the mechanism behind this result.

4. DISCUSSION

This study provides important practical insights on how the moisture level should be controlled throughout the CVD process to achieve highly consistent CNT forest growth, in terms of height and mass density. In the initial case I, where the presence of moisture as an impurity within gas tanks can cause significant moisture transients during the CVD process, we can attribute the significantly improved consistency for the decoupled recipe to the fact that withdrawal of the sample during the addition of C_2H_4 to the system allows the moisture level to stabilize before the sample is inserted. Cases II and III, wherein the atmosphere is kept dry and where a small amount of moisture is added, respectively, exhibit high consistency in both the reference and decoupled cases. Therefore, we can conclude that moisture fluctuations in the CVD process having magnitude of ∼10−100 ppm are detrimental to consistency and must be eliminated through reactor and process design. In Case IV, the catalyst is prepared under consistent dry conditions, while the moisture level in the reactor is well-controlled during growth at values up to 100s of ppm. Here, we find that the moisture content during the growth step influences the forest height kinetics, but not the apparent lifetime of the catalyst, as measured by the time of growth self-termination.

Moreover, an important difference between the decoupled and reference recipes is that the decoupled process introduces the substrate to the CVD chamber via rapid insertion, and as a result the catalyst is heated rapidly in the presence of the stabilized growth ambient. In cases II and III, where the moisture level is the same when comparing the decoupled and reference recipes, the higher CNT height and density obtained with the decoupled recipe suggest rapid heating of the catalyst (which has previously been annealed to form nanoparticles from the initial thin film) leads to a higher density of CNTs. This is also supported by the greater alignment (Hermans orientation parameter) measured when comparing results from the decoupled and reference recipes.

Therefore, albeit without more detailed mechanistic understanding at this point, we can conclude that rapid heating of the catalyst in the hydrocarbon environment improves the nucleation density of CNTs from the population of the catalyst particles. It may be hypothesized that rapid heating and hydrocarbon exposure leads to a greater uptake of carbon into the catalyst, allowing it to reach supersaturation needed for CNT nucleation, yet this requires further work and additional (ideally *in situ*) characterization. This is consistent with understanding that carbon supersaturation of the catalyst is necessary for nucleation,[30] and that CNT yield is influenced by the chemistry and concentration of the carbon source.[31]

Turning to the influence of the steady-state moisture concentration (case IV), we can conclude that the ratio of moisture to hydrocarbon in the CVD system influences the CNT forest growth kinetics. For example, Stadermann et al. reported that the best result for MWNT forest growth was achieved at a water/ethylene ratio of 1/330 (calculated from the ratio of partial pressures or flow rates of the pure vapors).[11] Futaba et al. found an optimal water/ethylene ratio of 1/1000 for large-diameter SWNT forests, reaching 800 μm after 10 min.[29] The maximum water/ethylene ratio we studied (case IV) is 1/370, which is comparable to Stadermann but is about 3 times higher than the optimal level reported by Futaba. From this, it can be concluded that the relative amounts of moisture and hydrocarbon influence the rate at which carbon is incorporated by and/or precipitated from the catalyst. Others have suggested that moisture can remove amorphous carbon at the catalyst,[28] though from our results it is apparent that the moisture concentrations we tested can increase the CNT growth rate, yet not extend the catalyst lifetime.

It is important to note that our approach did not permit investigation at concentrations below ∼1−10 ppm, yet others have shown that lower moisture levels and other oxygen-containing additives similarly influence CNT growth processes. For example, Wyss et al.[14] integrated gas purifiers to their growth system and eliminated impurities such as moisture, acetone, and O_2. When removing moisture to the sub-ppb level, they showed that CNT growth was prevented by high mobility and coarsening of Fe particles.

Last, we are able to draw conclusions from cases where the moisture level is kept identical during the annealing stage. Therefore, we can study the decoupled effect of moisture level on CNT growth during hydrocarbon exposure alone. Our previous work found that the moisture concentration during the annealing step influences the dewetting and migration of catalyst, which in turn influences the diameter and density of catalyst particles. Therefore, to precisely understand the influence of moisture on CNT growth kinetics, it is necessary to understand the effects of moisture on, and exercise separate control during, each stage of the process.

5. CONCLUSION

The findings of this study enable highly consistent synthesis of CNT forests under atmospheric pressure CVD conditions. This was achieved by decoupling the catalyst annealing and hydrocarbon exposures by movement of the sample in and out of the CVD system and stabilizing the moisture and hydrocarbon concentration between the two steps. First, we found that rapid insertion of the sample to this stable atmosphere leads to improved CNT density and forest height under all conditions. When the moisture level is controlled during the CNT growth step, yet kept to a constant baseline during annealing, we find that the controlled addition of moisture can improve the CNT forest growth rate, without influencing the CNT density or catalyst lifetime. This raises interesting questions regarding the roles of moisture in mediating CNT growth by CVD and shows that its role may be different during nucleation versus steady CNT growth.

■ ASSOCIATED CONTENT

Supporting Information

The Supporting Information is available free of charge on the ACS Publications website at DOI: 10.1021/acs.jpcc.6b02878.

Parameter table for decoupled recipe and reference recipe (Tables S1 and S2), schematic and photo of transfer arm sample loading system (Figure S1), carbon deposit coated on quartz tube (Figure S2), moisture control module (Figure S3), evolution of temperature during CVD process (Figure S4), AFM images of as annealed catalyst chip (Figure S5), TGA analysis of decoupled recipe produced forest (Figure S6), Raman

DOI: 10.1021/acs.jpcc.6b02878
J. Phys. Chem. C XXXX, XXX, XXX−XXX

spectra of CNT forests (Figure S7), SAXS analysis and imaging of CNT forest grown for 30 min by decoupled recipe (Figure S8), and probability density function of diameter distribution of CNT forest grown for 30 min by decoupled recipe (Figure S9) (PDF)

AUTHOR INFORMATION

Corresponding Author

*E-mail: ajhart@mit.edu.

Present Addresses

[§]Research Laboratory of Electronics (RLE), Massachusetts Institute of Technology, Cambridge, MA, 02139, USA.

[∥]Department of Mechanical Science and Engineering, University of Illinois, Urbana, IL 61801

Notes

The authors declare no competing financial interest.

ACKNOWLEDGMENTS

Financial support to J.L. and E.S.P. was provided by the National Science Foundation Scalable Nanomanufacturing Program (DMR-1120187) and a research grant from Pall Corporation, and financial support to A.O.W., S.T., and A.J.H. was provided by the Office of Naval Research Young Investigator Program (N000141210815). We thank Davor Copic and Kendall Teichert at the University of Michigan for assistance with catalyst deposition and LabVIEW programming, and Arthur Woll at Cornell University for assistance with X-ray scattering. Catalyst deposition was completed in the Lurie Nanofabrication Facility (LNF) at the University of Michigan. SEM and TEM characterizations were performed in the Electron Microbeam Analysis Laboratory (EMAL) at the University of Michigan. X-ray scattering was performed at the G1 beamline at the Cornell High-Energy Synchrotron Source (CHESS), which is supported by the National Science Foundation and the National Institutes of Health under Grant No. DMR-0225180.

REFERENCES

(1) Iijima, S.; Ajayan, P. M.; Ichihashi, T. Growth-model for carbon nanotubes. *Phys. Rev. Lett.* **1992**, *69*, 3100−3103.

(2) Hofmann, S.; Sharma, R.; Ducati, C.; Du, G.; Mattevi, C.; Cepek, C.; Cantoro, M.; Pisana, S.; Parvez, A.; Cervantes-Sodi, F.; et al. In-situ observations of catalyst dynamics during surface-bound carbon nanotube nucleation. *Nano Lett.* **2007**, *7*, 602−608.

(3) Meyyappan, M.; Delzeit, L.; Cassell, A.; Hash, D. Carbon nanotube growth by PECVD: A review. *Plasma Sources Sci. Technol.* **2003**, *12*, 205−216.

(4) Guo, T.; Nikolaev, P.; Thess, A.; Colbert, D. T.; Smalley, R. E. Catalytic growth of signle-walled nanotubes by laser vaporiztion. *Chem. Phys. Lett.* **1995**, *243*, 49−54.

(5) Hart, A. J.; Slocum, A. H. Rapid growth and flow-mediated nucleation of millimeter-scale aligned carbon nanotube structures from a thin-film catalyst. *J. Phys. Chem. B* **2006**, *110*, 8250−8257.

(6) Kataura, H.; Kumazawa, Y.; Maniwa, Y.; Ohtsuka, Y.; Sen, R.; Suzuki, S.; Achiba, Y. Diameter control of single-walled carbon nanotubes. *Carbon* **2000**, *38*, 1691−1697.

(7) Li, Y.; Liu, J.; Wang, Y. Q.; Wang, Z. L. Preparation of monodispersed Fe-Mo nanoparticles as the catalyst for CVD synthesis of carbon nanotubes. *Chem. Mater.* **2001**, *13*, 1008−1014.

(8) Cantoro, M.; Hofmann, S.; Pisana, S.; Scardaci, V.; Parvez, A.; Ducati, C.; Ferrari, A. C.; Blackburn, A. M.; Wang, K. Y.; Robertson, J. Catalytic chemical vapor seposition of single-wall carbon nanotubes at low temperatures. *Nano Lett.* **2006**, *6*, 1107−1112.

(9) Li, Q. W.; Zhang, X. F.; DePaula, R. F.; Zheng, L. X.; Zhao, Y. H.; Stan, L.; Holesinger, T. G.; Arendt, P. N.; Peterson, D. E.; Zhu, Y. T. Sustained growth of ultralong carbon nanotube arrays for fiber spinning. *Adv. Mater.* **2006**, *18*, 3160−3.

(10) Hata, K.; Futaba, D. N.; Mizuno, K.; Namai, T.; Yumura, M.; Iijima, S. Water-assisted highly efficient synthesis of impurity-free single-waited carbon nanotubes. *Science* **2004**, *306*, 1362−1364.

(11) Stadermann, M.; Sherlock, S. P.; In, J. B.; Fornasiero, F.; Park, H. G.; Artyukhin, A. B.; Wang, Y. M.; De Yoreo, J. J.; Grigoropoulos, C. P.; Bakajin, O.; et al. Mechanism and kinetics of growth termination in controlled chemical vapor deposition growth of multiwall carbon nanotube arrays. *Nano Lett.* **2009**, *9*, 738−744.

(12) Hasegawa, K.; Noda, S. Millimeter-tall single-walled carbon nanotubes rapidly grown with and without water. *ACS Nano* **2011**, *5*, 975−984.

(13) In, J. B.; Grigoropoulos, C. P.; Chernov, A. A.; Noy, A. Hidden role of trace gas impurities in chemical vapor deposition growth of vertically-aligned carbon nanotube arrays. *Appl. Phys. Lett.* **2011**, *98*, 153102.

(14) Wyss, R. M.; Klare, J. E.; Park, H. G.; Noy, A.; Bakajin, O.; Lulevich, V. Water-assisted growth of uniform 100 mm diameter SWCNT arrays. *ACS Appl. Mater. Interfaces* **2014**, *6*, 21019−21025.

(15) Zhang, G. Y.; Mann, D.; Zhang, L.; Javey, A.; Li, Y. M.; Yenilmez, E.; Wang, Q.; McVittie, J. P.; Nishi, Y.; Gibbons, J.; Dai, H. J. Ultra-high-yield growth of vertical single-walled carbon nanotubes: Hidden roles of hydrogen and oxygen. *Proc. Natl. Acad. Sci. U. S. A.* **2005**, *102*, 16141−16145.

(16) Amama, P. B.; Pint, C. L.; McJilton, L.; Kim, S. M.; Stach, E. A.; Murray, P. T.; Hauge, R. H.; Maruyama, B. Role of water in super growth of single-walled carbon nanotube carpets. *Nano Lett.* **2009**, *9*, 44−49.

(17) Oliver, C. R.; Polsen, E. S.; Meshot, E. R.; Tawfick, S.; Park, S. J.; Bedewy, M.; Hart, A. J. Statistical analysis of variation in laboratory growth of carbon nanotube forests and recommendations for improved consistency. *ACS Nano* **2013**, *7*, 3565−3580.

(18) Plata, D. L.; Meshot, E. R.; Reddy, C. M.; Hart, A. J.; Gschwend, P. M. Multiple alkynes react with ethylene to enhance carbon nanotube synthesis, suggesting a polymerization-like formation mechanism. *ACS Nano* **2010**, *4*, 7185−7192.

(19) Bedewy, M.; Meshot, E. R.; Guo, H. C.; Verploegen, E. A.; Lu, W.; Hart, A. J. Collective mechanism for the evolution and self-termination of vertically aligned carbon nanotube growth. *J. Phys. Chem. C* **2009**, *113*, 20576−20582.

(20) Wang, B. N.; Bennett, R. D.; Verploegen, E.; Hart, A. J.; Cohen, R. E. Characterizing the morphologies of mechanically manipulated multiwall carbon nanotube films by small-angle X-ray scattering. *J. Phys. Chem. C* **2007**, *111*, 17933−17940.

(21) Wang, B. N.; Bennett, R. D.; Verploegen, E.; Hart, A. J.; Cohen, R. E. Quantitative characterization of the morphology of multiwall carbon nanotube films by small-angle X-ray scattering. *J. Phys. Chem. C* **2007**, *111*, 5859−5865.

(22) Bedewy, M.; Meshot, E. R.; Reinker, M. J.; Hart, A. J. Population growth dynamics of carbon nanotubes. *ACS Nano* **2011**, *5*, 8974−8989.

(23) Meshot, E. R.; Verploegen, E.; Bedewy, M.; Tawfick, S.; Woll, A. R.; Green, K. S.; Hromalik, M.; Koerner, L. J.; Philipp, H. T.; Tate, M. W.; et al. High-speed in situ X-ray scattering of carbon nanotube film nucleation and self-organization. *ACS Nano* **2012**, *6*, 5091−5101.

(24) Pillai, S. K.; Ray, S. S.; Moodley, M. Purification of single-walled carbon nanotubes. *J. Nanosci. Nanotechnol.* **2007**, *7*, 3011−3047.

(25) Hou, P. X.; Liu, C.; Cheng, H. M. Purification of carbon nanotubes. *Carbon* **2008**, *46*, 2003−2025.

(26) Bedewy, M.; Meshot, E. R.; Hart, A. J. Diameter-dependent kinetics of activation and deactivation in carbon nanotube population growth. *Carbon* **2012**, *50*, 5106−5116.

(27) Kim, S. M.; Pint, C. L.; Amama, P. B.; Zakharov, D. N.; Hauge, R. H.; Maruyama, B.; Stach, E. A. Evolution in catalyst morphology leads to carbon nanotube growth termination. *J. Phys. Chem. Lett.* **2010**, *1*, 918−922.

DOI: 10.1021/acs.jpcc.6b02878
J. Phys. Chem. C XXXX, XXX, XXX−XXX

(28) Yamada, T.; Maigne, A.; Yudasaka, M.; Mizuno, K.; Futaba, D. N.; Yumura, M.; Iijima, S.; Hata, K. Revealing the secret of water-assisted carbon nanotube synthesis by microscopic observation of the interaction of water on the catalysts. *Nano Lett.* **2008**, *8*, 4288−4292.
(29) Futaba, D. N.; Hata, K.; Yamada, T.; Mizuno, K.; Yumura, M.; Iijima, S. Kinetics of water-assisted single-walled carbon nanotube synthesis revealed by a time-evolution analysis. *Phys. Rev. Lett.* **2005**, *95*, 4.
(30) Ding, F.; Bolton, K.; Rosen, A. Nucleation and growth of single-walled carbon nanotubes: A molecular dynamics study. *J. Phys. Chem. B* **2004**, *108*, 17369−17377.
(31) Kimura, H.; Goto, J.; Yasuda, S.; Sakurai, S.; Yumura, M.; Futaba, D. N.; Hata, K. Unexpectedly high yield carbon nanotube synthesis from low-activity carbon feedstocks at high concentrations. *ACS Nano* **2013**, *7*, 3150−3157.

DOI: 10.1021/acs.jpcc.6b02878
J. Phys. Chem. C XXXX, XXX, XXX−XXX